

On the Relevance of Mono- and Dinuclear Iron Carbonyl Complexes to the Fixation and Stepwise Hydrogenation of N₂^[‡]

Yu Chen,^[a] Michael Hartmann,^{*[a]} and Gernot Frenking^{*[a]}

Dedicated to Professor Dieter Sellmann on the occasion of his 60th birthday

Keywords: Ab initio calculations / Density functional theory / Iron / Carbonyl ligands / Nitrogen fixation / Hydrogenation

Density functional theory and high-level ab initio calculations are used to evaluate the influence of mono- and dinuclear iron carbonyl complexes to the fixation and stepwise hydrogenation of dinitrogen via diazene and hydrazine to ammonia. In comparison to the reaction of isolated N₂, only the first step in this reaction sequence (i.e. the reduction of N₂ to N₂H₂) experiences a significant change in its thermochemistry when coordinated to mono- or dinuclear iron tetracarbonyl fragments. The reaction enthalpy ΔH_R^0 ($T = 0$ K) for the endothermic hydrogenation of (CO)₄Fe–N₂ to give (CO)₄Fe–N₂H₂ is lower than for the corresponding metal-free process by 16.1 kcal mol^{–1}. The analogous step involving the dinuclear species (CO)₄Fe–N₂–Fe(CO)₄ and (CO)₄Fe–N₂H₂–Fe(CO)₄ is even less endothermic than the reduction involving only one iron tetracarbonyl complex by 13.1 kcal mol^{–1}. In comparison to that, the second and third step of this reduction sequence, namely the conversion of coordinated diazene to (CO)₄Fe–N₂H₄ and the subsequent reduction of coordinated hydrazine to (CO)₄Fe–NH₃ show only relatively small thermodynamic changes compared to the

analogous reactions of isolated N₂H₂ and N₂H₄. The reduction of (CO)₄Fe–N₂H₂ to (CO)₄Fe–N₂H₄ is almost as exothermic as the analogue reaction involving isolated N₂H₂, whereas the hydrogenation of (CO)₄Fe–N₂H₄ to (CO)₄Fe–NH₃ is less exothermic by 4.0 kcal mol^{–1}. Finally, the reduction of (CO)₄Fe–N₂H₂–Fe(CO)₄ and (CO)₄Fe–N₂H₄–Fe(CO)₄ are both predicted to be less exothermic than their mononuclear analogues by 4.0 and 1.1 kcal mol^{–1}, respectively. Moreover, we find that only N₂ and N₂H₂, which already show a noticeable π -acceptor behavior in their complexes with Fe(CO)₄, experience important structural changes in their corresponding dinuclear complexes, i.e. a shortening of the Fe–N bonds and a lengthening of the N–N bonds on going from (CO)₄Fe–L to (CO)₄Fe–L–Fe(CO)₄ (L = N₂, N₂H₂). This behavior is in line with a slightly increased π -acceptor ability of these ligands in their respective dinuclear complexes. Such structural changes are absent for N₂H₄, which only exhibits a comparatively weak π -acceptor character in (CO)₄Fe–N₂H₄.

Introduction

The stepwise hydrogenation of dinitrogen to ammonia is one of the most important processes in biochemical research^[1] and of utmost interest to chemical industry.^[2] Besides the well-understood heterogeneously catalyzed reduction following the Haber–Bosch process,^[3] deeper insight into the reduction of dinitrogen is necessary, particularly when dealing with biologically relevant systems. An example of this is the enzymatic fixation of N₂ catalyzed by nitrogenases.^[4] Although the molecular structure of the Fe–Mo cofactor of a nitrogenase enzyme has been characterized by X-ray structure analysis,^[5] details of the catalytically important features involved in the N₂ reduction have still not, however, been unequivocally answered.^[6] To

this end, the binding site, the binding mode of N₂ and the intermediates involved in the catalytic processes are still the source of much speculation.^[4,6]

It is widely accepted that the initial binding of dinitrogen occurs at the iron rather than the molybdenum centers.^[4] Theoretical studies based on different model systems of the Fe–Mo cofactor at various levels of theory are available.^[7] However, due to the complexity of the overall reduction process and the structure of the Fe–Mo cofactor, a suitable model system for the Fe–Mo nitrogenases that reasonably mimics its catalytic activity may be too large for a quantum chemical treatment at a reasonable level of theory.^[7] In addition to that, the nature of the actual intermediates of the enzymatic N₂ fixation process is still unknown.^[8] Although there are numerous results indicating that biological N₂ fixation involves diazene and hydrazine species,^[4] even the structure of the small four-atom diazene in solution was controversial until recently when Sellmann and Hennige isolated *trans*-N₂H₂ by complexation out of solution.^[9] Beside the clarification of the nature of the intermediates involved in the stepwise hydrogenation of N₂ by nitrogenases, another pivotal question regarding the thermochemistry of these reduction steps is of utmost interest: Sellmann and

[‡] Theoretical Studies of Inorganic Compounds, 14. – Part 13: Y. Chen, G. Frenking, *J. Chem. Soc., Dalton Trans.* **2001**, 434–440.

[a] Fachbereich Chemie, Philipps-Universität Marburg, Hans-Meerwein-Strasse, 35032 Marburg, Germany
Fax: (internat.) +49-6421/282-5566
E-mail: frenking@chemie.uni-marburg.de

Supporting information for this article is available on the WWW under <http://www.wiley-vch.de/home/eurjic> or from the author.

co-workers suggested that all of the three reduction steps involved in the hydrogenation sequence should benefit energetically from the coordination of the nitrogen-containing ligands to iron(II) sulfur complexes.^[6b]

Due to our interest in the structure and reactivity of iron carbonyl complexes,^[10] the present study focuses on the influence and relevance of mono- and dinuclear iron carbonyl complexes of the general type $[\{Fe(CO)_4\}_n L]$ ($n = 1$ for $L = NH_3$ and $n = 1, 2$ for $L = N_2, N_2H_2, N_2H_4$) to the fixation and stepwise hydrogenation of N_2 . We want to emphasize that this approach is not primarily intended to serve as a model study of the Fe–Mo cofactor, but to gain a deeper insight into the reduction steps of N_2 that are most affected by coordination to iron carbonyl fragments.^[6] Particular interest is thus drawn to thermodynamic changes between the “metalated” reaction in which the nitrogen-containing ligands are either coordinated by one or two iron tetracarbonyl fragments and the isolated, metal-free hydrogenation of N_2 . Moreover, we address the bonding situation of the Fe–L ($L = N_2, N_2H_2, N_2H_4$ and NH_3) bond in terms of σ -donor/ π -acceptor abilities and the preferred coordination site of the ligands.

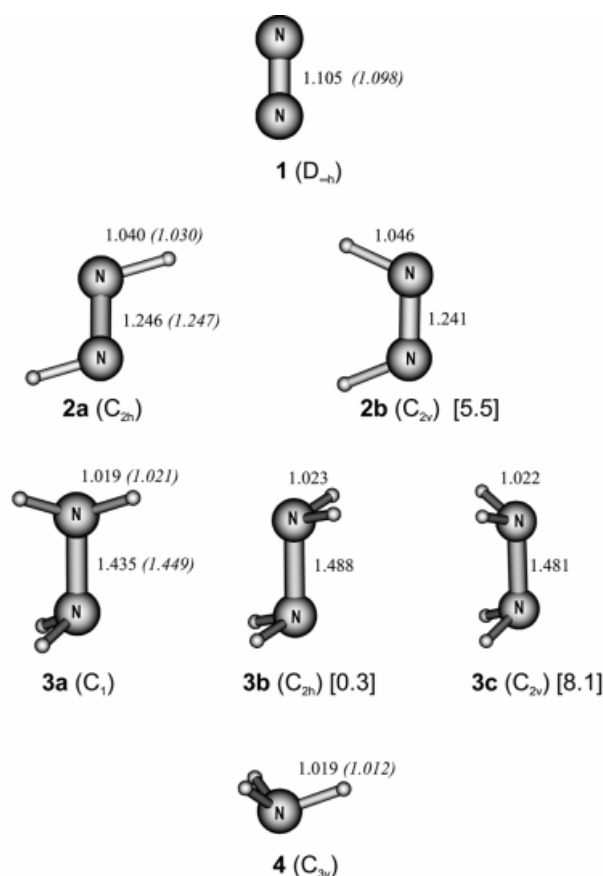


Figure 1. Optimized geometries of N_2 (1), N_2H_2 (2), N_2H_4 (3) and NH_3 (4); experimental values are given in italics; all bond lengths are in Å; the symmetry used for the geometry optimization is given in parentheses, while relative energies (kcal mol^{-1}) with respect to the most stable isomers are given in square brackets; angles are omitted for clarity and are provided separately in the Supplementary Information (Figure S1)

Results and Discussion

Stepwise Hydrogenation of Isolated Dinitrogen

The calculated geometries and structural parameters of dinitrogen **1**, diazene **2a** and **2b**, hydrazine **3a–3c** and ammonia **4** are shown in Figure 1. The reaction enthalpies obtained using a variety of energy evaluations based on the B3LYP/II geometries are summarized in Table 1. Details of the levels of theory necessary for a reasonable treatment of the stepwise hydrogenation of isolated dinitrogen to ammonia have been reported in a previous paper and the reaction enthalpies provided by this study serve as reference values for our present work.^[21] Thus, for the individual hydrogenation steps shown in Equations (1)–(3), the benchmarks for the reaction enthalpies ΔH_R^0 are $49.2 \text{ kcal mol}^{-1}$ [Equation (1)], $-23.1 \text{ kcal mol}^{-1}$ [Equation (2)] and $-44.7 \text{ kcal mol}^{-1}$ [Equation (3)].^[21]



Table 1. Hydrogenation enthalpies ΔH_R^0 (in kcal mol^{-1}) for the stepwise reduction of isolated dinitrogen^[a]

	$N_2 + H_2 \rightarrow N_2H_2$ (1)	$N_2H_2 + H_2 \rightarrow N_2H_4$ (2)	$N_2H_4 + H_2 \rightarrow 2 NH_3$ (3)
B3LYP/			
6–31G(d)	46.9	–18.0	–37.2
6–31G(d,p)	43.2	–19.6	–40.0
6–31+G(d,p)	43.3	–22.0	–43.3
6–31+G(2df,p)	44.1	–22.6	–43.4
6–31++G(2df,p)	44.1	–22.2	–43.1
6–311G(d,p)	47.1	–20.9	–41.6
6–311+G(d,p)	45.3	–22.4	–44.1
6–311+G(2df,p)	46.5	–22.0	–43.7
6–311++G(2df,p)	46.4	–22.0	–43.7
CCSD(T)			
6–31G(d)	55.8	–11.7	–37.3
6–31G(d,p)	49.1	–15.6	–41.6
6–311G(d,p)	44.1	–16.7	–41.7
6–311+G(d,p)	51.9	–18.3	–43.5
6–311+G(2df,p)	51.5	–19.3	–43.2
6–311++G(2df,p)	51.4	–19.3	–43.3
exp. ^[a]	49.2	–23.1	–44.7

[a] Ref. [21]

The data summarized in Table 1 clearly show that for all three hydrogenation steps convergence of the results is achieved when basis sets of at least 6–311+G(d,p) quality are used. At our highest level of theory, the enthalpies of reaction are $51.4 \text{ kcal mol}^{-1}$ for Equation (1), $-19.3 \text{ kcal mol}^{-1}$ for Equation (2) and $-43.3 \text{ kcal mol}^{-1}$ for Equa-

tion (3), which is in good agreement with the aforementioned reference data.^[21] We note, however, that the predicted ΔH_R^0 for the second reduction step [Equation (2)] is 3.8 kcal mol⁻¹ too high, while the reaction enthalpies of reactions (1) and (3) are too high by 2.2 and 1.4 kcal mol⁻¹, respectively. A more economic, yet reasonably accurate, alternative is given by CCSD(T) energy evaluations in combination with the 6-311+G(d,p) basis set. The deviations from the reference values are then between 4.8 and 1.2 kcal mol⁻¹, i.e. the ΔH_R^0 values are 51.9 kcal mol⁻¹ for Equation (1), -18.3 kcal mol⁻¹ for Equation (2) and -43.5 kcal mol⁻¹ for Equation (3). For larger molecules, for which CCSD(T) is no longer affordable, B3LYP/{II & 6-311+G(d,p)} single-point energies are recommended. This approach leads to deviations from the reference that are particularly small for reactions (2) and (3). The calculated ΔH_R^0 values of 45.3 kcal mol⁻¹ for Equation (1), -22.4 kcal mol⁻¹ for Equation (2) and -44.1 kcal mol⁻¹ for Equation (3) thus show that this approach offers a very economic way to reliable hydrogenation enthalpies.

The calculated N–N bond length of **1** is 1.105 Å, whereas the analogous bond lengths of **2a** and **2b** are calculated to be 1.246 and 1.241 Å, respectively. Compared to corresponding experimental data, the differences are quite small and in the range of 0.001 to 0.007 Å.^[22,23] The same also holds for the N–H bond length of NH₃ (**4**), that is, a small deviation from the experimental data by 0.007 Å is found.^[24] Relatively large deviations from the experimental values are, however, found for the structural parameters of **3a–3c**. The experimental N–N bond length of 1.449 Å is larger than the one we calculated for the most stable hydrazine isomer **3a** by 0.014 Å.^[24] Our calculated value is, however, in perfect agreement with other high-level ab initio estimates,^[21] implying that a re-examination of the experimental N–N bond length might be worthwhile. The calculated bond angles of **2**, **3** and **4** are generally in good agreement with the available literature data and we do not find significant deviations. Further details are given in the Supplementary Information (Figure S1).

At our standard level of theory, viz. CCSD(T)/II//B3LYP/II the *trans* isomer of diazene **2a** is predicted to be more stable than the *cis* isomer **2b** by 5.5 kcal mol⁻¹, which is in line with previous results.^[21,25] Furthermore, our calculations predict the *gauche* isomer **3a** to be the most stable form of hydrazine, which is consistent with other data.^[25] The energy difference to the corresponding *trans* isomer **3b** is, however, very small at only 0.3 kcal mol⁻¹, whereas the analogous *cis* hydrazine **3c** is significantly less stable than **3a** by 8.1 kcal mol⁻¹.

Stepwise Hydrogenation in the Presence of Mononuclear Iron Carbonyl Complexes

The influence of mononuclear iron carbonyl complexes on the stepwise hydrogenation of coordinated N₂ is evaluated by comparing the individual reduction steps shown in Equations (4)–(6) with their metal-free analogues in Equations (1)–(3).

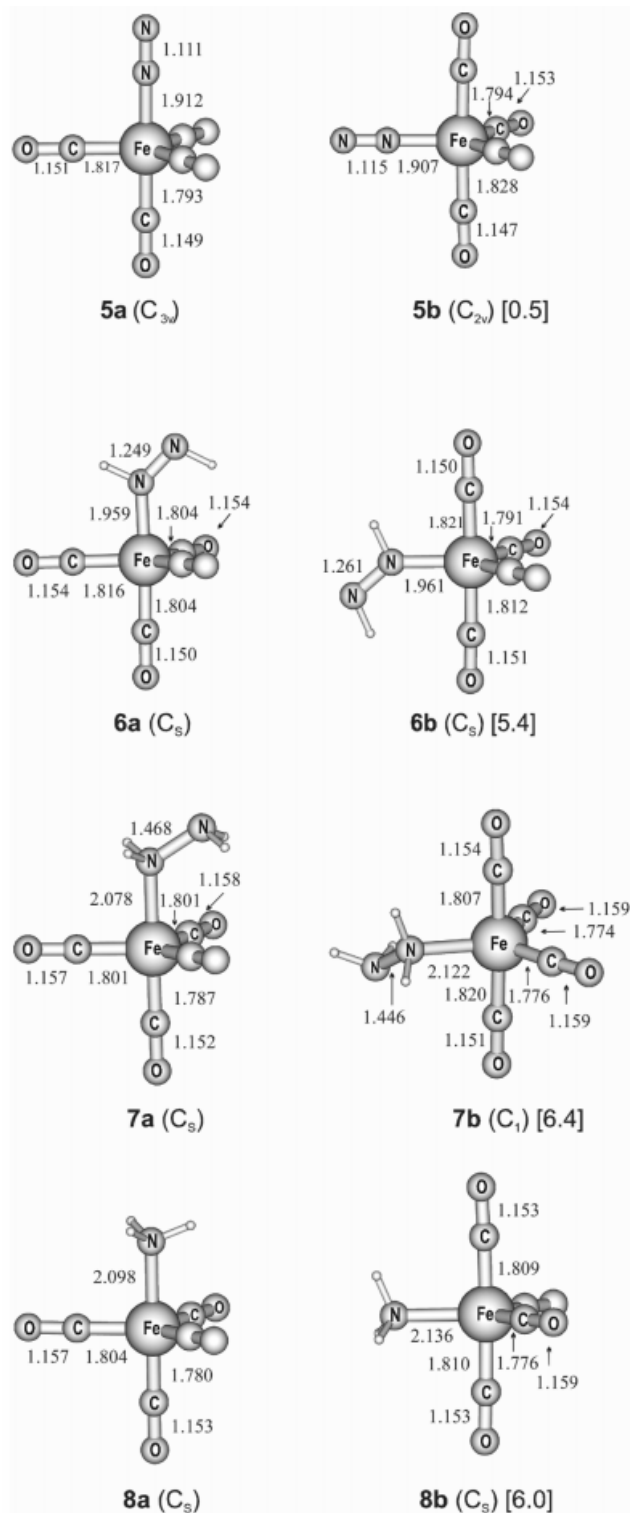
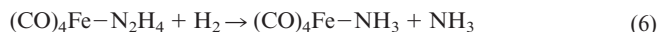
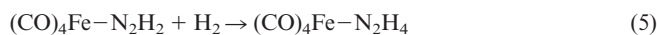
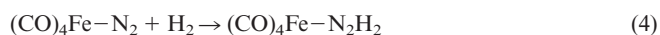


Figure 2. Optimized geometries of the complexes (CO)₄Fe–N₂ (**5**), (CO)₄Fe–N₂H₂ (**6**), (CO)₄Fe–N₂H₄ (**7**), and (CO)₄Fe–NH₃ (**8**); all bond lengths are in Å and the symmetry used for the geometry optimisation is given in parentheses; relative energies (kcal mol⁻¹) with respect to the most stable isomers are given in square brackets; angles and N–H bond lengths are omitted for clarity and are provided separately in the Supplementary Information (Figure S2)

Table 2. Hydrogenation enthalpies ΔH_R^0 (in kcal mol⁻¹) for the stepwise reduction of (CO)₄Fe–N₂^[a]

	(CO) ₄ FeN ₂ + H ₂ → (CO) ₄ FeN ₂ H ₂ (4)	(CO) ₄ FeN ₂ H ₂ + H ₂ → (CO) ₄ FeN ₂ H ₄ (5)	(CO) ₄ FeN ₂ H ₄ + H ₂ → (CO) ₄ FeNH ₃ + NH ₃ (6)
B3LYP			
6–31G(d)	32.4	–18.6	–35.4
6–31G(d,p)	30.7	–20.2	–38.8
6–311+G(d,p)	31.3	–20.4	–41.6
CCSD(T)			
6–31G(d)	39.2	–15.3	–33.4
6–31G(d,p)	35.9	–18.8	–39.0
6–311+G(d,p)	35.8	–18.5	–39.5

^[a] The basis sets given in the table refer to N and H, only. For all other main group elements the 6–31G(d) basis set is used.

The optimized geometries of the iron carbonyl complexes and the relative energies between the respective axial and equatorial isomers are shown in Figure 2. Table 2 summarizes the hydrogenation enthalpies ΔH_R^0 for Equations (4)–(6) obtained at various levels of theory. Table 3 lists the calculated bond dissociation energies D_0 between the Fe(CO)₄ fragment and the nitrogen-containing ligands together with the NBO and CDA data.

Table 3. Bond dissociation energies D_0 (kcal/mol) and NBO/CDA data for mononuclear iron tetracarbonyl complexes (CO)₄Fe–L obtained at the CCSD(T)/II//B3LYP/II level of theory

Complex	D_0	L	$q[\text{Fe}(\text{CO})_4]^{[b]}$	NBO ^[a]		CDA ^[a]	
				$q(\pi) \rightarrow \text{L}$	$q(\sigma) \rightarrow [\text{TM}]$	<i>b</i>	<i>d</i>
5a	22.9	N ₂	–0.08	0.18	0.26	0.14	0.28
6a	39.3	N ₂ H ₂	–0.18	0.15	0.33	0.10	0.30
7a	42.8	N ₂ H ₄	–0.29	0.10	0.39	0.03	0.36
8a	38.9	NH ₃	–0.27	0.13	0.40	–0.01	0.33

^[a] [TM] = [(CO)₄Fe]; $q(\sigma) \rightarrow [\text{TM}]$ σ -donation (*d*) and $q(\pi) \rightarrow \text{L}$ π -back donation (*b*) according to the NBO (CDA) analysis. – ^[b] Total charge of the Fe(CO)₄ complex fragment.

The most intriguing effect of the Fe(CO)₄ fragment on the stepwise hydrogenation of coordinated N₂ is that the enthalpy of hydrogenation of 35.8 kcal mol⁻¹ for the first reduction step [Equation (4)] is significantly lower by $\Delta\Delta H_R^0 = -16.1$ kcal mol⁻¹ compared to the analogous step of isolated N₂ [Equation (1)]. We do not observe a similarly drastic effect for the second and third reduction steps. To this end, the reduction of (CO)₄Fe–N₂H₂ [Equation (5)] is almost as exothermic as the corresponding hydrogenation [Equation (2)] of isolated N₂H₂ ($\Delta\Delta H_R^0 = -0.2$ kcal mol⁻¹). For the hydrogenation of (CO)₄Fe–N₂H₄ [Equation (6)], we even find a less exothermic behavior than for the metal-free analogue [Equation (3)] and $\Delta\Delta H_R^0$ is calculated to be 4.00 kcal mol⁻¹.

Dinitrogen is both a weak σ -donor and π -acceptor ligand. The small energy difference between the two possible isomers **5a** and **5b** of the complex (CO)₄Fe–N₂, in which N₂ is either coordinated axially or equatorially, implies no pronounced coordination site preference.^[26] The structures of **5a** and **5b** show Fe–N₂ bond lengths of 1.912 Å and

1.907 Å, respectively. This is in contrast to the results of Radius et al.,^[27] who predicted the Fe–N₂ bond length of axial N₂ to be shorter than that of equatorial N₂. The energy difference of 0.5 kcal mol⁻¹ between **5a** and **5b** is in favor of the axial isomer, which is again in contrast to the results of the aforementioned group.^[27] Note, however, that the chosen level of theory is surely beyond chemical accuracy (≤ 1.0 kcal mol⁻¹) and therefore our small energy difference is not conclusive. Interestingly, however, the uncertainty of the relative energy between **5a** and **5b** is also found in experimental chemistry. On the one hand, the reaction of Fe(CO)₅ with N₂ in polyethylene film implies that N₂ may occupy an equatorial rather an axial coordination site,^[28] whereas photolysis experiments of Fe(CO)₅ in nitrogen-containing matrices^[29] show an opposite behavior, that is, a more stable axial than equatorial isomer. The N–N distances of isomers **5a** and **5b** are both slightly longer than in isolated dinitrogen. The bond elongation upon coordination is in the range of 0.006 to 0.010 Å indicating that the N–N triple bond only experiences a weak “activation”. In addition, the calculated Fe–N bond energy of 22.9 kcal mol⁻¹ also implies a relatively weak interaction between N₂ and the Fe(CO)₄ fragment.

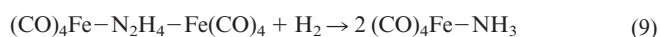
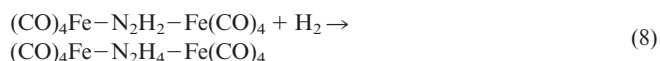
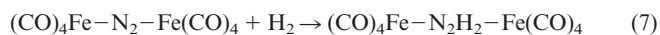
The diazene complex formed by the first hydrogenation step [Equation (4)] shows a somewhat different behavior than the analogous dinitrogen complex. First, the energy difference of 5.4 kcal/mol⁻¹ between the axial (**6a**) and equatorial (**6b**) isomers is indeed significant and in favor of the axial isomer. Second, this preference towards axial coordination is also mirrored by the σ -donor/ π -acceptor abilities of diazene.^[26] NBO as well as CDA data both imply that N₂H₂ is at least as poor a π -acceptor as N₂, but at the same time a slightly better σ -donor (Table 3). Finally, the Fe–N bond dissociation energy of **6a** is calculated to be 39.3 kcal mol⁻¹, which is considerably higher than the corresponding value calculated for **5a**. The much stronger bond in (CO)₄Fe–N₂H₂ than that in (CO)₄Fe–N₂ is the reason why the first hydrogenation step of N₂ becomes energetically more favored upon Fe(CO)₄ complexation. Any structural changes of diazene on complexation are again very small and the N–N bond is lengthened by only 0.003 Å.

Further hydrogenation of coordinated N₂H₂ leads to the corresponding hydrazine complex [Equation (5)]. NBO and CDA data suggest that hydrazine is a significantly stronger σ -donor than diazene or dinitrogen (Table 3). Axial coordination of N₂H₄ should therefore be predominant, which is supported by the large energy difference of 6.4 kcal mol⁻¹ that favors the axial isomer **7a** over its equatorial analog **7b**. Interestingly, the former, more stable, isomer has hydrazine coordinated as *trans*-N₂H₄, which is not the most stable conformation for the isolated case. At the same time, the less-stable equatorial isomer has N₂H₄ coordinated in its most stable *gauche* conformation. Structural changes of N₂H₄ on coordination are significant as shown by the lengthening of the N–N bond in **7a** by 0.033 Å with respect to isolated N₂H₄. This relatively strong influence on the internal structure of N₂H₄ is also mirrored by the large Fe–N bond dissociation energy of 42.8 kcal mol⁻¹, which is, in fact, the highest *D*₀ value encountered in this study. Note, that at the same time the calculated Fe–N bond length of **7a** of 2.078 Å is significantly larger than the corresponding bond lengths found in complexes **5** and **6**, which exhibit weaker bonds between iron and the nitrogen-containing ligands.

In the final step [Equation (6)] of the overall reduction process, coordinated hydrazine is reduced to ammonia. The NH₃ ligand is found by CDA and NBO to be an equally strong σ -donor as N₂H₄, whereas its π -acceptor capability is close to zero (Table 3). Again we find a dominant preference of the axial (CO)₄Fe–N₂ isomer **8a** over the equatorial isomer by 6.0 kcal mol⁻¹, which is in line with crystallographic data and IR spectra.^[30] Our estimate for the Fe–N bond dissociation energy is 38.9 kcal mol⁻¹ and the calculated Fe–N bond length is 2.098 Å. Both values show slight deviations from those found for the analogous hydrazine complex **7a**. These differences are, however, small, thus indicating a close resemblance of these two complexes.

Stepwise Hydrogenation in the Presence of Dinuclear Iron Carbonyl Complexes

Figure 3 shows the optimized geometries of the dinuclear iron tetracarbonyl complexes (CO)₄Fe–N₂–Fe(CO)₄ (**9**), (CO)₄Fe–N₂H₂–Fe(CO)₄ (**10**) and (CO)₄Fe–N₂H₄–Fe(CO)₄ (**11**), considered in the hydrogenation steps according to Equations (7)–(9). Table 4 and 5 summarize the hydrogenation enthalpies for the individual steps and the bond dissociation energies, as well as the NBO/CDA data, respectively.



The coordination of dinitrogen by two iron tetracarbonyl fragments results in a further significant decrease of the hydrogenation enthalpy of the first reduction step [Equation (7)] by $\Delta\Delta H_R^0 = -13.1$ kcal mol⁻¹ compared to the analogous step [Equation (4)] involving only one Fe(CO)₄

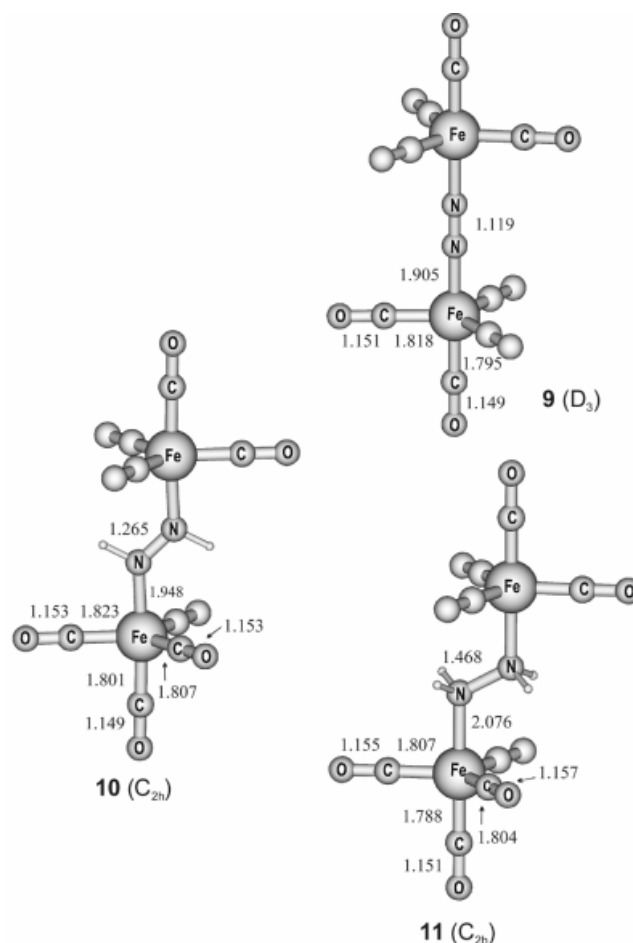


Figure 3. Optimized geometries of the dinuclear iron tetracarbonyl complexes (CO)₄Fe–N₂–Fe(CO)₄ (**9**), (CO)₄Fe–N₂H₂–Fe(CO)₄ (**10**), and (CO)₄Fe–N₂H₄–Fe(CO)₄ (**11**); all bond lengths are in Å; the symmetry used for the geometry optimization is given in parentheses; for more details regarding structural parameters see the Supporting Information (Figure S3)

fragment.^[31] The overall decrease of the hydrogenation enthalpy with respect to the metal free reaction [Equation (1)] thus becomes 27.1 kcal mol⁻¹.^[31] This considerable change of the thermochemistry is so much more interesting as it only affects the first reduction step. To this end, the second [Equation (8)] and third [Equation (9)] hydrogenation steps are even less exothermic than their mononuclear analogues [Equation (5) and (6)]. The $\Delta\Delta H_R^0$ values calculated on going from Equation (5) to (8) and from Equation (6) to (9) are 4.0 and 1.1 kcal mol⁻¹, respectively.

The Fe(CO)₄ fragments in **9** are twisted against each other by 8.7°. The rotation barrier is extremely low and we find several different isomers that are energetically not distinguishable from each other. In comparison to the mononuclear analogue **5a** we do not observe further significant alterations of structural parameters. Note that the Fe–N bond length becomes shorter by 0.007 Å, which is paralleled by the lengthening of the N–N bond by 0.008 Å. The CDA and NBO data in Table 5 show that the σ -donor properties of N₂ embraced by two iron tetracarbonyl fragments is hardly changed compared to **5a** — only the π -

Table 4. Hydrogenation enthalpies ΔH_R^0 (in kcal mol⁻¹) for the stepwise reduction of (CO)₄Fe–N₂–Fe(CO)₄^[a]

	$[(\text{CO})_4\text{Fe}]_2\text{N}_2 + \text{H}_2 \rightarrow$ $[(\text{CO})_4\text{Fe}]_2\text{N}_2\text{H}_2$ (7)	$[(\text{CO})_4\text{Fe}]_2\text{N}_2\text{H}_2 + \text{H}_2 \rightarrow$ $[(\text{CO})_4\text{Fe}]_2\text{N}_2\text{H}_4$ (8)	$[(\text{CO})_4\text{Fe}]_2\text{N}_2\text{H}_4 + \text{H}_2 \rightarrow$ $2(\text{CO})_4\text{FeNH}_3$ (9)
B3LYP			
6–31G(d)	19.9	–16.2	–39.2
6–31G(d,p)	17.6	–17.0	–42.0
6–311+G(d,p)	18.2	–16.4	–40.5

^[a] The basis set given in the table refers to N and H, only. All of the other elements use the 6–31G(p) basis set.

Table 5. Bond dissociation energies D_0 (kcal/mol) and NBO/CDA data for dinuclear iron tetracarbonyl complexes (CO)₄Fe–L–Fe(CO)₄ obtained at the B3LYP/II//B3LYP/II level of theory

Complex	$D_0^{[b]}/D_0^{[c]}$	L	$q[\text{Fe}(\text{CO})_4]^{[d]}$	NBO ^[a]		CDA ^[a]	
				$q(\pi) \rightarrow \text{L}$	$q(\sigma) \rightarrow [\text{TM}]_2$	<i>b</i>	<i>d</i>
9	16.0/32.5	N ₂	–0.05	0.40	0.50	0.28	0.50
10	28.6/59.6	N ₂ H ₂	–0.11	0.38	0.60	0.24	0.57
11	26.1/57.7	N ₂ H ₄	–0.24	0.18	0.66	0.11	0.63

^[a] [TM] = [(CO)₄Fe]; $q(\sigma) \rightarrow [\text{TM}]$ σ -donation (*d*) and $q(\pi) \rightarrow \text{L}$ π -back donation (*b*) according to the NBO (CDA) analysis with respect to both Fe(CO)₄ fragments. Half of this value equals the charge transferred per Fe(CO)₄ unit. – ^[b] Fe–L bond dissociation energy per Fe(CO)₄ fragment according to: [TM]₂L → [TM]L + TM. – ^[c] Total Fe–L bond dissociation energy according to: [TM]₂L → TM + TM + L. – ^[d] Total charge of the Fe(CO)₄ complex fragment.

acceptor characteristics are somewhat enhanced. The overall Fe–N₂–Fe bond dissociation energy is calculated to be 32.5 kcal mol⁻¹, which translates to a Fe–N bond dissociation energy per Fe(CO)₄ fragment of 16.0 kcal mol⁻¹. Comparison of these data with the bond dissociation energy obtained for **5a** implies a decreased bond strength between an individual Fe(CO)₄ subunit and N₂.

Further hydrogenation of **9** results in the formation of the corresponding diazene complex (CO)₄Fe–N₂H₂–Fe(CO)₄ (**10**). The Fe–N as well as the N–N bond lengths of **10** are calculated to be 1.948 Å and 1.265 Å, respectively. These values are in good agreement with the structural data of the related [μ–N₂H₂{Fe(PPR₃)('S₄')}]₂ [³² S₄'^{2–} = 1,2-bis(2-mercaptophenylthio) ethane(2-)] complex reported by Sellmann and co-workers.^[32] The small deviations of less than 0.052 Å are noteworthy as such Fe^{II}('S₄') complexes involving multidentate organosulfur ligands are often used as model compounds for the Fe–Mo, Fe–V and Fe–Fe nitrogenases.^[4,6,32] We note a non-negligible shortening of the Fe–N bond by 0.011 Å and a lengthening of the N–N bond by 0.016 Å on going from **6a** to its dinuclear pendant **10**. Interestingly, CDA and NBO data indicate that the ability of diazene to act as σ -donor is almost unaltered. Only a slight increase of the π -acceptor capabilities of N₂H₂ is observed. The Fe–N bond dissociation energy of **10** follows the same trend as shown above for the corresponding dinitrogen complex; that is, the bond strength per Fe(CO)₄ fragment is smaller than in the mononuclear case, whereas the overall binding energy obtained by complexation with two Fe(CO)₄ fragments is significantly larger.

In the second step of the overall reduction process [Equation (8)], the analogous hydrazine complex

(CO)₄Fe–N₂H₄–Fe(CO)₄ (**11**) is formed by hydrogenation of coordinated diazene. The comparison with complex **7a** shows hardly any shortening of the Fe–L bond length or lengthening of the N–N bond. We want to point out that the NBO data imply that both the σ -donor as well as the π -acceptor abilities of N₂H₄ decrease slightly on going from the mononuclear complex to **11**. With respect to the σ -donor character this is also supported by the corresponding CDA values. Although the analogue π -acceptor value implies a stronger π back-donation of N₂H₄ in the dinuclear complex **11**, the predicted magnitude is too small to account for a significant π -acceptor character of N₂H₄.

Conclusion

Density functional and ab initio calculations were used to evaluate the influence of iron tetracarbonyl complexes on the stepwise hydrogenation of dinitrogen. In comparison to the metal-free reduction process, we find that complexation by one or two Fe(CO)₄ fragments results in a pronounced change of the thermochemistry of the first hydrogenation step, namely the reduction of coordinated N₂ to N₂H₂. The effects on the second and third hydrogenation steps, viz the hydrogenation of coordinated N₂H₂ and N₂H₄, are much weaker, and even less-exothermic reduction processes compared with the metal-free hydrogenation are predicted. The decrease of the hydrogenation enthalpy is larger for the reduction of (CO)₄Fe–N₂–Fe(CO)₄ than it is for the reduction of (CO)Fe–N₂. In conclusion, our calculations thus clearly demonstrate that only one, namely the first, reduction step in the hydrogenation sequence of N₂ is

in fact favored in terms of the reaction enthalpy by complexation with iron tetracarbonyl fragments. Although the systems used in our study are not intended to primarily serve as model complexes for the mode of action of nitrogenase, we suggest that these results should be considered in further discussions of the thermochemistry of N₂ fixation and activation processes.

The binding characteristics of N₂, N₂H₂, N₂H₄ and NH₃ to Fe(CO)₄, analyzed in terms of the NBO and CDA partitioning schemes, imply a consistent trend of the σ -donor/ π -acceptor behavior of these ligands that correlates with the relative energies between the respective isomers. Thus, ligands with comparatively high σ -donor capabilities like N₂H₄ and NH₃ give iron tetracarbonyl complexes in which the axial isomers are considerably more stable than their equatorial analogues. In addition to that, only ligands like N₂ and N₂H₂ that show noticeable π -acceptor quantities in their respective Fe(CO)₄ complexes are affected by the formation of dinuclear complexes. Thus, the Fe–N bond lengths are shorter and the N–N bonds are longer in the dinuclear complexes than in their mononuclear analogues. This behavior is also mirrored by a slight increase of the π -acceptor ability on going from (CO)₄Fe–X to (CO)₄Fe–X–Fe(CO)₄ (X = N₂, N₂H₂) complexes. Such structural changes are absent for N₂H₄, and both its σ -donor as well as its π -acceptor behavior are less pronounced in (CO)₄Fe–N₂H₄–Fe(CO)₄ than in (CO)₄Fe–N₂H₄.

Experimental Section

Computational Details: Geometry optimizations were performed with Becke's three-parameter hybrid functional in combination with the correlation functional according to Lee, Yang and Parr (B3LYP).^[11] A small core pseudopotential and a (441/2111/41) split-valence basis set according to Hay and Wadt were used for iron,^[12] whereas an all-electron 6–31G(d) basis set was chosen for the main-group elements.^[13] It was shown previously that this combination of basis sets (further abbreviated as basis set II) in combination with the aforementioned functional predicts equilibrium geometries of transition metal complexes reasonably well.^[14] All structures discussed in this paper were verified to represent local minima on their potential energy surfaces by harmonic frequency calculations at the same level of theory. Refined estimates of relative energies were obtained by single-point calculations of the B3LYP/II geometries using both the B3LYP functional and coupled-cluster theory with singles, doubles and perturbative estimates of triple substitution [CCSD(T)].^[15] CCSD(T) and basis set II were used for estimating relative energies between isomeric forms of diazene, hydrazine and all iron carbonyl complexes. Refined reaction enthalpies ΔH_R^0 (T = 0 K) for the individual hydrogenation reactions, however, were predicted using basis sets that consisted of the aforementioned basis set for the metal and the elements C and O, but were extended by either the 6–31G(d,p) or the 6–311+G(d,p) basis sets for N and H. These combinations of basis sets are further abbreviated as {II & 6–31G(d,p)} and {II & 6–311+G(d,p)}, respectively.

The ΔH_R^0 values obtained for the hydrogenation steps of the metal-free reactions were compared with their analogous steps involving mononuclear iron carbonyl fragments. The resulting $\Delta\Delta H_R^0$ values

indicate whether the ΔH_R^0 of an individual reduction step decreases ($\Delta\Delta H_R^0 < 0$) or increases ($\Delta\Delta H_R^0 > 0$) on going from the reactions of the isolated to the coordinated species. The corresponding $\Delta\Delta H_R^0$ values obtained for the individual reduction steps involving mono- and dinuclear iron carbonyl fragments were used likewise. Unless otherwise noted, relative enthalpies obtained at the CCSD(T)/{II & 6–311+G(d,p)}/B3LYP/II level of theory were the basis for the comparison between the metal-free hydrogenation steps of N₂ and the reactions following the reduction of (CO)₄Fe–N₂. With respect to the large resources needed for a proper description of the reactions involving dinuclear species, the comparisons between the hydrogenation steps involving mono and dinuclear iron carbonyl complexes were based on the B3LYP/{II & 6–311+G(d,p)}/B3LYP/II energies only. For the evaluation of the reaction enthalpies only the most stable isomers within a reaction sequence were considered.

Reaction enthalpies and relative energies are corrected by zero-point vibrational energy (ZPE) contributions obtained at the B3LYP/II level of theory. The nature of the Fe–N and N–N bonds was examined using the natural bond orbital (NBO)^[16] partitioning scheme and the charge decomposition analysis (CDA).^[17] All calculations used the program packages Gaussian94/98,^[18] MOLPRO96/2000,^[19] and CDA2.1.^[20]

Acknowledgments

This work was supported by the Deutsche Forschungsgemeinschaft (DFG) and the Fonds der Chemische Industrie. Excellent help by the computer center of Philipps-Universität Marburg is gratefully acknowledged. Additional computer time was provided by the HLRZ Darmstadt, Frankfurt and Giessen and the HLR Stuttgart and is hereby acknowledged.

- [1] [1a] J. Kim, D. C. Rees, *Biochemistry* **1994**, *33*, 389. – [1b] P. E. M. Siegbahn, M. R. A. Blomberg, *Chem. Rev.* **2000**, *100*, 421–438.
- [2] K. H. Büchel, H.-H. Moretto, P. Woditsch, *Industrielle Anorganische Chemie 3rd edition*, Wiley-VCH, Weinheim, **1999**.
- [3] See, for example: [3a] *Catalytic Ammonia Synthesis: Fundamentals and Practice Vol. I* (Ed.: J. R. Jennings), Plenum, New York, **1991**. – [3b] F. A. Cotton, G. Wilkinson, C. A. Murillo, M. Bochmann, *Advanced Inorganic Chemistry 6th edition*, Wiley-Interscience, **1999**, 316–318.
- [4] For recent reviews, see: [4a] J. B. Howard, D. C. Rees, *Chem. Rev.* **1996**, *96*, 2965–2982. – [4b] B. K. Burgess, D. J. Lowe, *Chem. Rev.* **1996**, *96*, 2983–3012. – [4c] R. R. Eady, *Chem. Rev.* **1996**, *96*, 3013–3030 [4d] M. D. Fryzuk, S. A. Johnson, *Coord. Chem. Rev.* **2000**, *200–202*, 379–409.
- [5] [5a] J. Kim, D. C. Rees, *Science* **1992**, *257*, 1677. – [5b] J. Kim, D. C. Rees, *Nature* **1992**, *360*, 553–560.
- [6] [6a] D. Sellmann, J. Sutter, *Acc. Chem. Res.* **1997**, *30*, 460–469. – [6b] D. Sellmann, J. Utz, N. Blum, F. W. Heinemann, *Coord. Chem. Rev.* **1999**, *190–192*, 607–627. – [6c] D. Sellmann, A. Fürsattel, J. Sutter, *Coord. Chem. Rev.* **2000**, *200–202*, 545–561.
- [7] [7a] B. C. Machado, E. R. Davidson, *Theor. Chim. Acta* **1995**, *92*, 315326. – [7b] I. Dance, *Chem. Commun.* **1996**, 165–166. – [7c] I. Dance, *Chem. Commun.* **1998**, 523–530.
- [8] G. E. Koch, K. C. Schneider, R. H. Burris, *Biochem. Biophys. Acta* **1960**, *37*, 273–279.
- [9] D. Sellman, A. Hennige, *Angew. Chem.* **1997**, *109*, 270–271; *Angew. Chem. Int. Ed. Engl.* **1997**, *36*, 276.
- [10] See, for example: [10a] A. W. Ehlers, G. Frenking, *Organometallics* **1995**, *14*, 423–426. – [10b] M. Torrent, M. Sola, G. Frenking, *Organometallics* **1999**, *18*, 2801–2812.

- [11] [11a] A. D. Becke, *J. Chem. Phys.* **1993**, *98*, 5648–5652. — [11b] C. Lee, W. Yang, R. G. Parr, *Phys. Rev.* **1988**, *B37*, 785–789.
- [12] P. J. Hay, W. R. Wadt, *J. Chem. Phys.* **1985**, *82*, 299–310.
- [13] [13a] J. A. Pople, R. Krishnan, H. B. Schlegel, J. S. Binkley, *Int. J. Quantum Chem.* **1978**, *14*, 545–560. — [13b] R. J. Bartlett, G. D. Purvis, *Int. J. Quantum Chem.* **1978**, *14*, 561–581. — [13c] G. D. Purvis, R. J. Bartlett, *J. Chem. Phys.* **1982**, *76*, 1910–1918. — [13d] G. D. Purvis, R. J. Bartlett, *J. Chem. Phys.* **1987**, *86*, 7041–7050.
- [14] G. Frenking, I. Antes, M. Böhme, S. Dapprich, A. W. Ehlers, V. Jonas, A. Neuhaus, M. Otto, R. Stegmann, A. Veldkamp, S. F. Vyboishchikov, in *Reviews in Computational Chemistry*, Vol. 8 (Eds.: K. B. Lipkowitz and D. B. Boyd), VCH, New York, **1996**, 63–144.
- [15] [15a] J. Cizek, *J. Chem. Phys.* **1966**, *45*, 4256–4266. — [15b] J. Cizek, *Adv. Chem. Phys.* **1969**, *14*, 35–89.
- [16] A. E. Reed, L. A. Curtiss, F. Weinhold, *Chem. Rev.* **1988**, *88*, 899–926.
- [17] S. Dapprich, G. Frenking, *J. Phys. Chem.* **1995**, *99*, 9352–9362.
- [18] [18a] Gaussian 94, Revision D.4, M. J. Frisch, G. W. Trucks, H. B. Schlegel, P. M. W. Gill, B. G. Johnson, M. A. Robb, J. R. Cheeseman, T. Keith, G. A. Petersson, J. A. Montgomery, K. Raghavachari, M. A. Al-Laham, V. G. Zakrzewski, J. V. Ortiz, J. B. Foresman, J. Cioslowski, B. B. Stefanov, A. Nanayakkara, M. Challacombe, C. Y. Peng, P. Y. Ayala, W. Chen, M. W. Wong, J. L. Andres, E. S. Replogle, R. Gomperts, R. L. Martin, D. J. Fox, J. S. Binkley, D. J. Defrees, J. Baker, J. P. Stewart, M. Head-Gordon, C. Gonzalez, and J. A. Pople, Gaussian, Inc., Pittsburgh PA, **1995**. — [18b] Gaussian 98, Revision A.3, M. J. Frisch, G. W. Trucks, H. B. Schlegel, G. E. Scuseria, M. A. Robb, J. R. Cheeseman, V. G. Zakrzewski, J. A. Montgomery, Jr., R. E. Stratmann, J. C. Burant, S. Dapprich, J. M. Millam, A. D. Daniels, K. N. Kudin, M. C. Strain, O. Farkas, J. Tomasi, V. Barone, M. Cossi, R. Cammi, B. Mennucci, C. Pomelli, C. Adamo, S. Clifford, J. Ochterski, G. A. Petersson, P. Y. Ayala, Q. Cui, K. Morokuma, D. K. Malick, A. D. Rabuck, K. Raghavachari, J. B. Foresman, J. Cioslowski, J. V. Ortiz, B. B. Stefanov, G. Liu, A. Liashenko, P. Piskorz, I. Komaromi, R. Gomperts, R. L. Martin, D. J. Fox, T. Keith, M. A. Al-Laham, C. Y. Peng, A. Nanayakkara, C. Gonzalez, M. Challacombe, P. M. W. Gill, B. Johnson, W. Chen, M. W. Wong, J. L. Andres, C. Gonzalez, M. Head-Gordon, E. S. Replogle, and J. A. Pople, Gaussian, Inc., Pittsburgh PA, **1998**.
- [19] MOLPRO is a package of ab initio programs written by H.-J. Werner and P. J. Knowles, Universität Stuttgart and University of Birmingham.
- [20] CDA 2.1, S. Dapprich, G. Frenking, Marburg, **1994**. The Program is available via anonymous ftp at: <ftp://ftp.chemie.uni-marburg.de/pub/cda>.
- [21] S. Sekusak, G. Frenking, *J. Mol. Struct., Theochem*, in print.
- [22] H. Herzberg, *Molecular Spectra and Molecular Structure, Part I – Spectra of Diatomic Molecules 2nd ed.*, Krieger Publishing Co., Malabar, Florida, **1989**.
- [23] J. Demaison, F. Hegelund, H. Bürger, *J. Mol. Struct.* **1997**, *413–414*, 447–456.
- [24] *CRC Handbook of Chemistry and Physics 76th Ed.* (Ed.: D. R. Lide), **1995–1996**.
- [25] [25a] J. A. Pople, L. A. Curtiss, *J. Chem. Phys.* **1991**, *95*, 4385–4388. — [25b] M. L. McKee, D. M. Stanbury, *J. Am. Chem. Soc.* **1992**, *114*, 3214–3219.
- [26] Experimental data and qualitative molecular orbital considerations imply that strong π -accepting ligands prefer equatorial coordination sites of trigonal bipyramidal complexes of d^8 metals, whereas σ -donor ligands prefer axial coordination sites. See, for example: [26a] A. R. Rossi, R. Hoffmann, *Inorg. Chem.* **1975**, *14*, 365–374. — [26b] J. K. Burdett, *Inorg. Chem.* **1976**, *15*, 212–219. — [26c] M. C. Favas, D. L. Kepert, *Prog. Inorg. Chem.* **1980**, *27*, 325463. [26d] D. P. Bauer, J. K. Ruff, *Inorg. Chem.* **1983**, *22*, 1686–1689. [26e] D. B. Beach, S. P. Smit, W. L. Jolly, *Organometallics* **1984**, *3*, 556–559. — [26f] T. A. Albright, J. K. Burdett, M. H. Whangbo, *Orbital Interactions in Chemistry*, Wiley: New York, **1985**, pp 324–325.
- [27] U. Radius, F. M. Bickelhaupt, A. W. Ehlers, N. Goldberg, R. Hoffmann, *Inorg. Chem.* **1998**, *37*, 1080–1090.
- [28] A. I. Cooper, M. Poliakoff, *Chem. Phys. Lett.* **1993**, *212*, 611–616.
- [29] [29a] M. Poliakoff, J. J. Turner, *J. Chem. Soc., Dalton Trans.* **1974**, 2276–2285. — [29b] M. Poliakoff, *Chem. Soc. Rev.* **1978**, 527–540.
- [30] F. A. Cotton, J. M. Troup, *J. Am. Chem. Soc.* **1974**, *96*, 3438–3443.
- [31] Note the levels of theory used for this comparison. Reaction enthalpies of reduction steps following $(\text{CO})_4\text{Fe}-\text{N}_2-\text{Fe}(\text{CO})_4$ use the B3LYP/{II + 6–311+G(d,p)}/B3LYP/II combination of methods.
- [32] D. Sellmann, H. Friedrich, F. Knoch, M. Moll, *Z. Naturforsch., Teil B* **1994**, *49*, 76–88.

Received October 12, 2000

[100388]